Development and Running Control of a 3D Leg Robot

Takayuki IKEDA[1], Tetsuya TAMURA[1] and Tsutomu MITA[1]

[1]Department of Control and Systems Engineering
Tokyo Institute of Technology
2-12-1, Ohokayama, Meguro-ku, Tokyo 152-0033, Japan
ikeda@ctrl.titech.ac.jp

Abstract

In this research work, we will develop a 3D biped which simulates running motion of human. First, we will explain the mechanism of our 3D biped (Runbot 2). Next, we will show that the running motion pattern for the biped can be approximated by solutions of second or first order differential equations. Then we will derive a control strategy of the running biped which realizes these differential equations as motion pattern. Simulation results suggest that a biped having smooth running gait will be realized.

1. Introduction

In [1]-[3], we have developed three planar robots (Runbot-A, Runbot-B and Runbot-C) and succeeded to derive a control method such that they can run in the two dimensional space. In this paper, we will develop a control methodology of a biped which can run in the three-dimensional space by extending the mechanism and control of the previous results.

Static and dynamic walking have been realized using different and unique techniques by many researchers [4], [5], [6], [7], [8]. Several fundamental ideas toward realizing walking robots have been proposed in these research works. For example, the concept of ZMP and control technique based on the inverted pendulum were examined to obtain a control law which prevents turnover [4]. However, since the walking motion and running motion are really different from the viewpoint of speed and balancing, we think that a running motions are not obtained by direct applications of the results in these research works.

In particular, it is well known that Raibert and his group have created a running biped and quadruped using translated legs with spring action [9]. Although their results were very excellent, we think that it is not direct to switch the modes of the motions among walk, run and jump smoothly. To realize a walking robot moving supplely like living animals, we need to build running robots using articular joints. However, it is also difficult to extend and apply Raibert's results to running robots with articular joints since his result has been derived depending upon several ideal conditions of the mechanism, e.g, the leg motion does not affect the motion of the body.

The main reasons of the difficulties are considered to be the following: (1) The mechanism suitable for running has not been well investigated. This includes the actuation problem. (2) There is no effective control theory for the robot which can run. Raibert's results may restrict mechanisms as mentioned above.

In this paper, as a basic research work toward creating running biped composed of all articular joints, we will introduce our new running biped (Runbot 2) and propose a method which potentially control its running motion in 3D space. In order to simplify the control systems design, we assume that the three-dimensional movement of the biped can be decomposed into three motions in sagittal, lateral and horizontal planes. As the control strategy, the variable constraint control [1] is introduced. In this control, the motion patterns which the biped follows are described by differential equations. Several simulation results show that we can control Runbot 2.

2. Mechanism design and equation of motion

We will deal with a running biped depicted in Fig.1. Since direct analysis and design of the biped in 3D space is too complicated, we will introduce a coordination system shown in Fig.2 and assume that the running motion of the robot can be decomposed into three planar motions, i.e., motions in YOZ plane, XOZ plane and XOY plane which are known as the sagittal-plane, lateral-plane and horizontal-plane, respectively. In reality, each motion may interfere. In this research work, we will deal with such interference force as disturbances added to the control loops and we expect that they are controlled by our control strategy shown below.

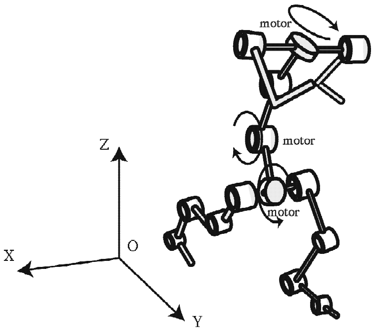

Figure 1: 3D biped robot

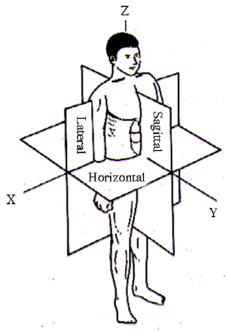

Figure 2: Axis and plains

2.1. Mechanism design of Runbot2

The three-dimensional biped Runbot2 (humanoid type) shown in Fig.1 was developed in our research lab this year. The configuration of the joints and actuators are shown in Fig.1. Fig. 3 shows the variables of the robot in the sagittal-plane; Fig. 4 and Fig.5 explain those in the lataral-plane and horizontal-plane, respectively. The overview of the designed Runbot2 is shown in Fig. 6.

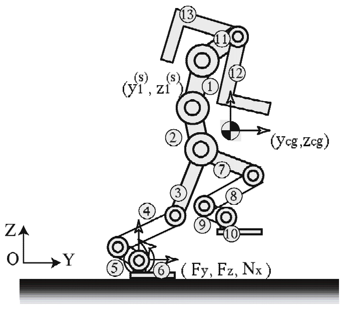

Figure 3: Sagital plane

The mechanism design has been done by taking the following assumptions and conditions into considerations.

[1] The motion in the sagittal-plane will be controlled by eight actuators of the both legs.

[2] The motion in the lateral-plane will be controlled by one waist actuator.

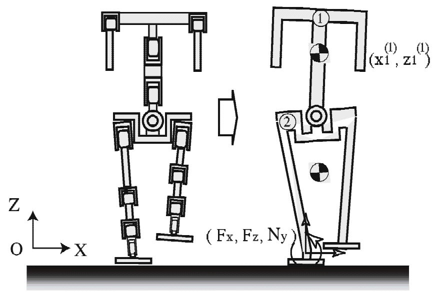

Figure 4: Lateral plane

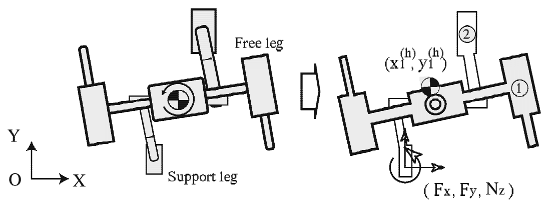

Figure 5: Horizontal plane

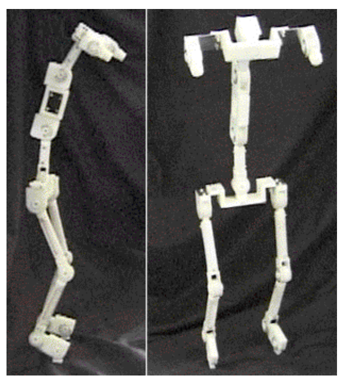
Figure 6: Runbot2 (humanoid type)

[3] The motion in the horizontal-plane will be controlled by one of the backbone actuator.

[4] The posture of the leg at the touchdown moment is selected to obtain the best manipulability.

[5] The foot toe will contact the surface.

[6] The shoulders are added as redundant DOF's.

The reason for the item [1] is that we will control the four fundamental characteristic variables shown below plus four joint angles of the swinging leg independently, just the same as the previous work [1]

Since we think that the motions in lateral and horizontal planes are not essential for the running, we have simply introduced the items [2] and [3].

In another previous work [3], we found that the concept of the manipulability of the leg posture at the touchdown moment is very important to reduce the magnitude of required force to keep running. This is the reason for the item [4]. Such a care is never taken for the mechanism introduced by Raibert.

The assumption in the item [5] makes the formulation of the motion and real control easier. Runbot2 has the force sensors at the foot toe to judge contact condition.

The shoulders in the item [6] are introduced for a future work. In the current research, the actuators of shoulders are not used.

2.2. The equation of motion of Runbot2

The motion in the saggital-plane will be described by 13 links and 12 joints as depicted in Fig. 3. The motion in the lateral-plane will be described by 2 link and 1 joint as depicted in Fig. 4. The motion in the horizontal-plane will be described by 2 link and 1 joint as depicted in Fig. 5.

Supposing that the robot does not jump long and its attitude can be recovered during the touchdown period, we only deal with the touchdown phase which starts from the landing of the toe and ends up with its lift-off. In this interval, the toe is assumed to be fixed, and the tip of foot and the absolute angle of the foot are kept zero. This leads to the following equation of motion [10], [11]:

$$M(q)\ddot{q} + h(q,\dot{q}) = \phi_q^T(q)\lambda + f_q^T(q)u \qquad (1)$$

$$\ddot{\phi}(q) + C\dot{\phi}(q) + K\phi(q) = 0 \qquad (2)$$

where $q(t) \in R^n$ is the generalized coordinates; $u(t) \in R^m$ is the control torques; $M(q)$ is inertia matrix; $h(q,\dot{q})$ is the gravity, centrifugal force and Coriolis force terms; $\phi(q) \in R^3$ is the position of the toe and the absolute angle of the foot; $\lambda(t) \in R^3$ is the force required to maintain the contact $\phi(q) = 0$ and is expressed in term of the Lagrange multiplier; $\phi_q = \frac{\partial \phi}{\partial q}$ gives the direction of the constraint force; $f_q = \frac{\partial f}{\partial q}$ is the Jacobian matrix which converts the direction of the input.

If we assume that $C > 0, K > 0$, $\phi(q_0) = 0$, $\dot{\phi}(q_0) = 0$, the constraint $\phi(q) = 0$ be expressed by (2).

The matrix and vector in the equation (1) and (2Åj are composed of the following matrix and vector, respectively.

$$q := \begin{bmatrix} u^{(s)} \\ q^{(\ell)} \\ q^{(h)} \end{bmatrix}, \quad u := \begin{bmatrix} q^{(s)} \\ u^{(\ell)} \\ u^{(h)} \end{bmatrix}, \quad ,\lambda := \begin{bmatrix} \lambda^{(s)} \\ \lambda^{(\ell)} \\ \lambda^{(h)} \end{bmatrix}$$

$$h := \begin{bmatrix} h^{(s)} \\ h^{(\ell)} \\ h^{(h)} \end{bmatrix}, \quad f := \begin{bmatrix} f^{(s)} \\ f^{(\ell)} \\ f^{(h)} \end{bmatrix}, \quad ,\phi := \begin{bmatrix} \phi^{(s)} \\ \phi^{(\ell)} \\ \phi^{(h)} \end{bmatrix}$$

$$M := diag([M^{(s)}, M^{(\ell)}, M^{(h)}]) \;,$$
$$C := diag([C^{(s)}, C^{(\ell)}, C^{(h)}]) \;,$$
$$K := diag([K^{(s)}, K^{(\ell)}, K^{(h)}])$$

where, index(s) and (ℓ), (h) mean the sagittal-plane, lateral-plane and horizontal-plane, respectively.

3. Control of the motion pattern via VCC

We will derive the control law which gives desired motion pattern to the motion of the biped described by (1) and (2). We assume that the required motion pattern of the robot is expressed by the following differential equation.

$$\ddot{\zeta}(t) = \eta(\zeta(t), \dot{\zeta}(t)) \qquad (3)$$

where $\zeta(t) \in R^k$ is called characteristic variables which express the motion of the robot. We will show the method to generate $\zeta(t)$ in the next section.

We can confirm that $\dot{\zeta}(t)$ is expressed by a function of the generalized velocity $\dot{q}$ as

$$\dot{\zeta} = g_q(q)\dot{q}, \qquad (4)$$

and (3) can also be written as

$$g_q(q)\ddot{q} + \dot{g}_q(q)\dot{q} + C\{\dot{\zeta}(t) - \dot{\bar{\zeta}}(t)\} + K\{\zeta(t) - \bar{\zeta}(t)\} = 0, \qquad (5)$$

if we want to derive the acceleration term $\ddot{q}$ explicitly.

Then arranging (1), (2) and (5) yield

$$\begin{bmatrix} M(q) & -\phi_q^T & -f_q \\ -\phi_q & 0 & 0 \\ -g_q & 0 & 0 \end{bmatrix} \begin{bmatrix} \ddot{q} \\ \lambda \\ u \end{bmatrix} = \begin{bmatrix} -h(q,\dot{q}) \\ \dot{\phi}_q\dot{q} + C\dot{\phi}(q) + K\phi(q) \\ \dot{g}_q(q)\dot{q} + \eta(\zeta,\dot{\zeta}) \end{bmatrix} \qquad (6)$$

Solving (6) leads to

$$\begin{bmatrix} \lambda \\ u \end{bmatrix} = \left\{ \begin{bmatrix} \phi_q \\ g_q \end{bmatrix} M^{-1} \begin{bmatrix} \phi_q^T & f_q^T \end{bmatrix} \right\}^{-1}$$
$$\left\{ \begin{bmatrix} \phi_q \\ g_q \end{bmatrix} M^{-1} h + \begin{bmatrix} -\dot{\phi}_q \dot{q} - C\phi_q \dot{q} - K\phi \\ -\dot{g}_q \dot{q} - \eta(\zeta, \dot{\zeta}) \end{bmatrix} \right\} \quad (7)$$

The existence condition of the control is that the matrix inside $\{\ \}^{-1}$ in (7) is of full row rank which can be satisfied in the present case since the mechanism is full actuated. As long as the constraint force λ can be supplied from the floor, the response of the closed loop system exactly simulates (3) since (7) is the decoupling control by regarding ζ as the output to follow. We call have called this control strategy as the *variable constraint control (VCC)* in [1].

3.1. Running motion pattern

In this section, we will derive three running motion patterns for the three planar motions.

3.2. Running motion pattern in the sagittal-plane

At the touchdown phase, we must control the kicking and balancing motions of the robot in the sagittal-plane. In this research work, we have paid attention to the following four fundamental *characteristic variables*;

[C1] y_{cg} [C2] z_{cg} [C3] L_{cg_x} [C4] L_{a_x}

where (y_{cg},z_{cg}) is the position of CG of the whole robot; L_{cg_x} is the total angular momentum with respect to CG of the total robot; L_{a_x} is the total angular momentum with respect to the toe.

In order to verify these arguments and derive the time response of C1∼C4, we have analyzed [1] the running motion of human using the sequence photographs [14] as shown in Fig. 7, Fig. 8 and Fig. 9.

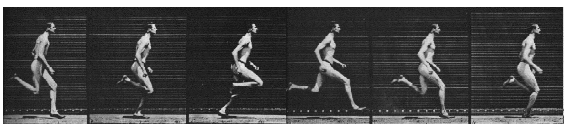

Figure 7: Consecutive photograph of human

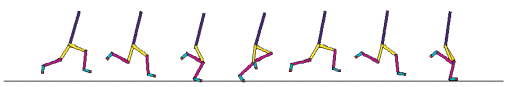

Figure 8: Motion of human

From this analysis, we have concluded that the motion of the CG of running human can be approximated

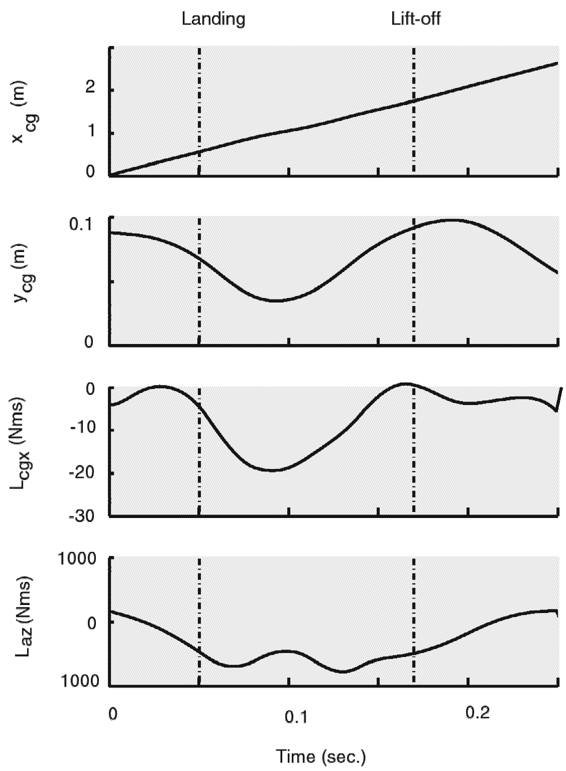

Figure 9: Center of gravity and Angular momentum

by a bouncing ball phenomenon. And the response of L_{cg_x} is described such that once becomes negative at the beginning of the touchdown and recovers to zero before the lift-off by regarding the first peak as an initial disturbance. The angular momentum L_{a_x} is just the same as L_{cg_x} except for the steady state. The steady state $\bar{L}_{a_x}$ of L_{a_x} is given by a nonzero value which means that the CG of the robot rotates after touchdown and the ZMP moves from the heel to the toe before the lift-off [1].

We modeled the motion pattern in the sagittal-plane as follows.

$$m\ddot{y}_{cg} + c_y\{\dot{y}_{cg} - \dot{\bar{y}}_{cg}\} + k_y\{y_{cg} - \bar{y}_{cg}\} = 0 \quad (8)$$
$$m\ddot{z}_{cg} + c_z\{\dot{z}_{cg} - \dot{\bar{z}}_{cg}\} + k_z\{z_{cg} - \bar{z}_{cg}\} = 0 \quad (9)$$
$$\dot{L}_{cg_x} + c_{cg_x} L_{cg_x} = 0 \quad (10)$$
$$\dot{L}_{a_x} + c_{a_x}\{L_{a_x} - \bar{L}_{a_x}\} = 0 \quad (11)$$

where $\bar{y}_{cg}(t) = \bar{v}t + y_{cg-}$, $\bar{z}_{cg}(t) = z_{cg-}$; (y_{cg-}, z_{cg-}) is the position of CG at the starting time t_- of the touchdown phase; $\bar{v}$ is the average speed of the velocity during the touchdown; k_y and k_z are spring coefficients; $c_{cg_x} > 0$ and $c_{a_x} > 0$ are damping coefficients.

We will control the posture of the swinging leg by regarding its four joint angles as additional characteristic variables of four dimensional, that is:

[C5-C8] $\hat{\theta} = [\theta_7, \theta_8, \theta_9, \theta_{10}]$

The posture is chosen to have the best manipulability in the next touchdown moment and is simply represented by

$$\bar{\theta} = [\bar{\theta}_7, \bar{\theta}_8, \bar{\theta}_9, \bar{\theta}_{10}] \tag{12}$$

Then, the motion pattern for the swinging leg is given by the following differential equation.

$$\ddot{\hat{\theta}} + C_{\hat{\theta}}\dot{\hat{\theta}} + K_{\hat{\theta}}\{\hat{\theta} - \bar{\theta}\} = 0 \ , \ C_{\hat{\theta}} > 0 \ , \ K_{\hat{\theta}} > 0 \tag{13}$$

We will control y_{cg}, z_{cg}, L_{cg_x}, L_{a_x} and $\theta_7 - \theta_{10}$ by eight actuators of both legs.

3.3. Running motion pattern in the lateral-plane

We will control the balance in the lateral-plane to keep the center of gravity to the toe center x_a. Then, the characteristic variable in the lateral-plane is defined as follows.

[C9] The center of gravity position x_{cg}

When we approximate the motion pattern of x_{cg} as that $x_{cg}(t) \rightarrow x_a$, it can be described as

$$\ddot{x}_{cg}(t) + c_x\dot{x}_{cg}(t) + k_x\{x_{cg}(t) - x_a\} = 0, \tag{14}$$

where $c_x > 0$ and $k_x > 0$.

3.4. Running motion pattern in the horizontal-plane

We think that the balance in the horizontal-plane is just like the above. In this case, the characteristic variable is chosen as

[C10] The horizontal angular momentum around the CG, L_{cg_z}

And the motion pattern is given by the differential equation

$$\dot{L}_{cg_z}(t) + c_{cg_z}L_{cg_z}(t) = 0, \tag{15}$$

where $c_{cg_z} > 0$ is chosen to simulate the decay rate.

3.5. Total running motion pattern

Equation(8), (9), (10), (11), (13), (14) and (15) yield

$$\ddot{\zeta}(t) + \tilde{C}\{\dot{\zeta}(t) - \dot{\bar{\zeta}}(t)\} + \tilde{K}\{\zeta(t) - \bar{\zeta}(t)\} = 0, \tag{16}$$

when we define

$$\zeta(t) = [x_{cg}(t), y_{cg}(t), z_{cg}(t), \int_0^t L_{cg_x}(\tau)d\tau, \int_0^t L_{cg_z}(\tau)d\tau, \int_0^t L_{a_x}(\tau)d\tau, \hat{\theta}]^T. \tag{17}$$

Then substituting the derived ζ into (3) yields the variable constraint control for the running biped.

3.6. Simulation results

When an initial velocity is given to the robot, it can run several steps. The responses of the characteristic variables concerned with sagittal and lateral, horizontal plane are shown in 10, Fig. 11 and Fig. 12. These results show that a biped robot may be produced which has smooth running gaits. Stick diagram of the motion of the robot is shown in Fig. 13, Fig. 14 and Fig. 15.

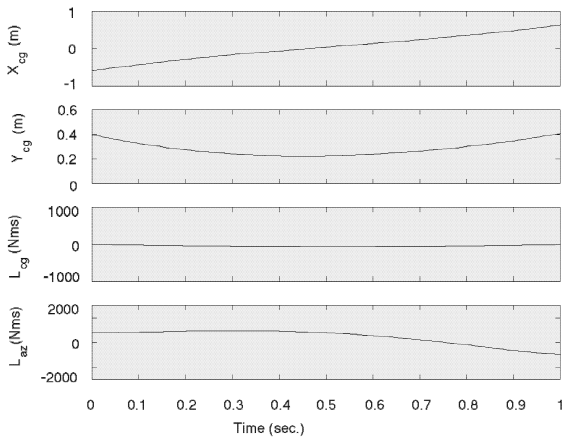

Figure 10: Simulation result (Sagittal Plane)

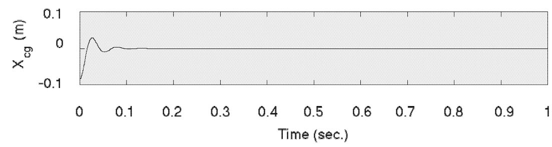

Figure 11: Simulation result (Lateral Plane)

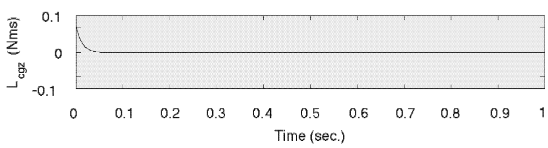

Figure 12: Simulation result (Horizontal Plane)

4. Conclusions

We have explained the mechanism of our 3D biped, Runbo2. We also have derived the running motion pattern for the biped and proposed a control strategy which can realize the running motion pattern. Simulation results suggest that a biped potentially can be produced which has smooth running gaits. We are now installing the experimental system and expect the positive results. Future research work includes realizing

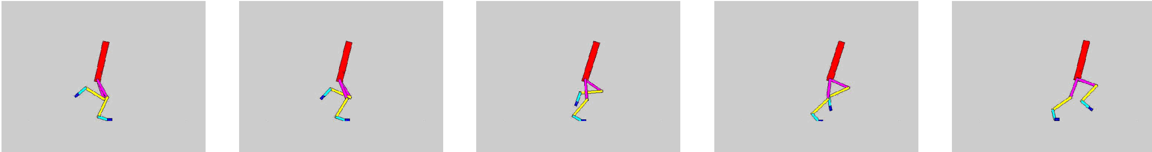

(a) t = 0.0 (sec.) (b) t = 0.2 (sec.) (c) t = 0.4 (sec.) (d) t = 0.6 (sec.) (e) t = 0.8 (sec.)

Figure 13: Stick diagram (Sagittal Plane)

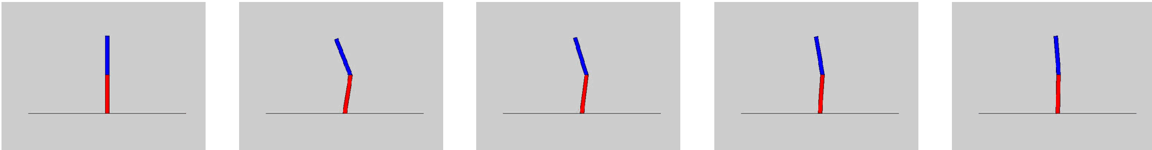

(a) t = 0.0 (sec.) (b) t = 0.2 (sec.) (c) t = 0.4 (sec.) (d) t = 0.6 (sec.) (e) t = 0.8 (sec.)

Figure 14: Stick diagram (Lateral Plane)

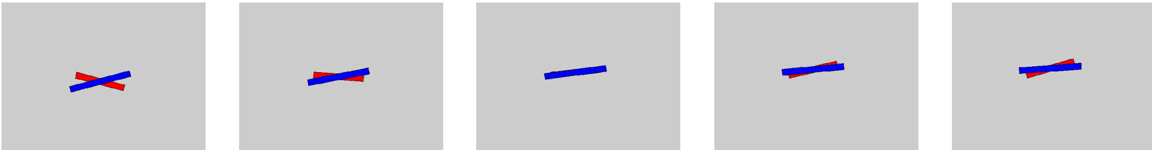

(a) t = 0.0 (sec.) (b) t = 0.2 (sec.) (c) t = 0.4 (sec.) (d) t = 0.6 (sec.) (e) t = 0.8 (sec.)

Figure 15: Stick diagram (Horizontal Plane)

quadruped robots in the three-dimensional space using the proposed control strategy.

5. Acknowledgement

This research work is carried out using the COE grant (COE: Super Mechano-Systems) supported by the Japanese Ministry of Education, Science, Culture and Sports.

References

[1] T. Ikeda, Y. Iwatani, K. Suse, T.Mita : Analysis and Design of Running Robots in Touchdown Phase, Proc. of CCA99, pp. 496-501 (1999)

[2] T. Mita, T. Ikeda, K. Suse, Y. Iwatani: Design of a quadruped robot which can run and jump –Basic analysis and control systems design–, IEEE Hong Kong Sympo. on Robotics and Control, July 2nd, pp. 393-398 1999.

[3] T. Ikeda, T. Mita: Posture Design of Running Robot based on Dynamic Manipulability, The 22th SICE Symposium on Dynamical System Theory (in Japanese), (1999)

[4] J. Yamaguchi, A. Takanishi, and I. Kato: ”Development of a Biped Walking Robot Compensating for Three-Axis Moment by trunk Motion,” Proceedings of the 1993 IEEE/RSJ Int. Conf. on Intelligent Robots and System pp. 561-566 (1993)

[5] Honda: http://www.honda.co.jp/english /technology/robot/index.html

[6] J. Furusho, M. Masubuchi : ”Control of a D ynamical Biped Locomotion System for Steady Walking,” Trans. ASME, J.of Dyn. Sys. Mes.and Control, vol. 108, no. 2, pp. 111-118 (1986)

[7] S. Kajita, K. Tani : ”Experimental Study of Bipe d Dynamics Walking,” IEEE Control Systems, vol. 16, no. 1, pp. 13-19 (1996)

[8] H. Kimura et al. ,Dynamic walking and running of the quadruped using neural oscillator, Proc. of IEEE &RSJ IROS98, pp.50-57, 1998.

[9] M. H. Raibert:” Legged Robots That Balance,” MIT Press, Cambridge, Massachusetts (1985)

[10] E. J. Haug: Computer-Aided Kinematics and Dynamics of Mechanical Systems. vol. 1, Basic Methods, Allyn and Bacon (1989)

[11] A. A. Shabana: Dynamics of Multibody Systems. Cambridge Univ. Pr. (1998)

[12] R. Margaria: Biomechanics and Energetics of Muscular Exercise. Oxford University Press (1976)

[13] M. Vukobratovic, B. Borovac, D. Surla, D. Stokic: Biped Locomotion - Dynamics, Stability, Control and Application - . Springer-Verlag (1990)

[14] E. Muybridge: Animals in motion. Dover (1957)